Research Article

Journal of Environmental Nanotechnology

Effect of Al_2O_3 Nanofiller on the Mechanical Performance of Hemp-kenaf Reinforced Epoxy Hybrid Composites

B. Nanthini[1], S. Seenivasan[2*], T. Prabhu[1], Kelin S. Johnson[1], V. Sathya[1] and M. Jegadeeswaran[1]

[1]Department of Agricultural Engineering, Rathinam Technical Campus, Coimbatore, TN, India
[2]Department of Mechanical Engineering, Rathinam technical campus, Coimbatore, TN, India
Received: 30.07.2025 Accepted: 29.09.2025 Published: 30.09.2025
*kannanarchieves@gmail.com

ABSTRACT

Biocompatibility, affordability, and broad availability are three reasons why natural-based composites are gaining popularity among both producers and consumers. The possibility of forming a composite with alumina (Al_2O_3) a cost-effective nano filler material, natural fibers, and an epoxy matrix is explored in this study. In particular, it investigates the effects of three different Al_2O_3 concentrations on the mechanical properties of a hybrid composite made of hemp and kenaf, including hardness, impact resistance, flexural strength, and inter-laminar shear strength (ILSS). Hand layup followed by hot pressing was used to produce the composites. The composite containing 6 wt% Al_2O_3 (C3) outperformed the other configurations by a margin of 2% to 36 % in terms of tensile, flexural, ILSS, and impact strengths. Adding 6 wt% Al_2O_3 increased the mechanical properties of the composite by increasing fiber-matrix adhesion, according to scanning electron microscopy (SEM) study of the cracked surfaces.

Keywords: Impact strength; Flexural strength; Inter-laminar shear strength; Mechanical properties; Natural fibers.

1. INTRODUCTION

Concerns about the environment and the advantages of natural fibers over synthetic alternatives have recently propelled natural fiber reinforced polymer composites (FRPs) to the forefront of worldwide attention. For composite applications, researchers are looking into a variety of natural fibers, each with its own set of advantages and disadvantages. These include ramie, kenaf, flax, hemp, sisal, coir, bagasse, and jute. Composites made from natural fibers have many benefits, including being biodegradable (especially when used with a biodegradable matrix), cost-effective, and reducing CO_2 emissions during production. Natural fibers like flax and jute improve the mechanical properties of polymer matrices, such as their tensile, flexural, impact, and interlaminar shear strengths. Environmental aspects are implied through the use of natural fiber as a sustainable reinforcement. A recent study promotes green composite development by reducing dependence on synthetic fibers (Subbiah *et al.* 2024). Environmental concern is central, with the development of green composites for industrial applications (Harak *et al.* 2024). The use of natural fibers combined with nanoparticles aims to enhance wear resistance while maintaining sustainability. Another study has contributed to environmentally friendly material development for packaging and automotive sectors (Mayakannan *et al.* 2023). NaOH alkali treatment was used for up to 12 hours to improve fiber surface properties and interfacial bonding. A recent work reported the fabrication of eco-friendly hybrid composites using biodegradable fibers and recyclable nano-fillers (Edlabadkar *et al.* 2025). Biotex flax/PLA epoxy composites were markedly enhanced following treatment with 5% NaOH, attributable to the incorporation of Al_2O_3 and MgO nanofillers (Amjad *et al.* 2021).

PLA-based green composites were crushed and reinforced using hemp fibers. Their antibacterial properties augment their use in biomedicine, resulting in a smaller environmental footprint, and are superior to biodegradability (Raj *et al.* 2025). Eco-friendly composites were fabricated utilizing hand lay-up and curing at 110°C, incorporating sun hemp fiber mats (Alshahrani and Prakash, 2024). Krishna *et al.* (2022) demonstrated that the length and orientation of the fibers influence the mechanical performance of eco-friendly materials. Epoxy composites reinforced with NaOH-treated groundnut shell and luffa fibers, incorporating Al_2O_3 fillers at concentrations between 5% and 15%. Thirty percent fiber and ten percent aluminium oxide yielded the most favorable outcomes (Kumar *et al.* 2024). Composites of sun hemp, carbon/E-glass layers and 3 wt% nano-silica enhanced impact resistance, and tensile strength. Eco-friendly automotive composites exhibited effective interfacial bonding as evidenced by FESEM (Bharathi *et al.* 2021). Hybrid composites including jute, kenaf, and glass fibers with Al_2O_3 nanoparticles (3-5

wt%) exhibited improved tensile and impact strength (Arunachalam *et al.* 2025). Sun hemp, flax, sisal, and rosin served as fillers in hybrid epoxy composites, enhancing hardness, impact resistance, and tensile strength. Various rosin-flax composites exhibited superior performance under mechanical stress (John *et al.* 2020).

The incorporation of Al_2O_3 into glass (G) fiber composites with *Prosopis juliflora* (J) enhanced their mechanical properties. The JJGGJJJGGG sequence surpassed all in impact, flexural, and tensile properties (Rakeshkumar *et al.* 2023). The flexural strength and tensile strength of epoxy composites reinforced with cashew shell biosilica and satin-woven sun hemp were 204 MPa and 164 MPa, respectively (Jayabalakrishnan *et al.* 2024). Composites composed of areca fiber and epoxy containing varying proportions of Al_2O_3 (from 0 to 8 wt%), shows enhanced mechanical properties. SEM analyses of the NaOH-treated fibers demonstrated a uniform dispersion of Al_2O_3 and robust adhesion between the fibers and the matrix (Tavadi *et al.* 2025). Composites including aluminium and bamboo stem ash powder (BSAP) exhibited improved mechanical properties at 7.5 wt% BSAP, featuring a hardness of 239.66 HV and a compressive strength of 308.32 MPa (Haile *et al.* 2024). Al_2O_3 and MgO nanofillers were employed to enhance Jute fiber epoxy bio-nanocomposites, both with and without NaOH treatment. At a concentration of 3 wt% nanofillers, the mechanical properties such as compressive and interlaminar shear strength, were maximized (Amjad *et al.* 2022). Epoxy, rice husk, Al_2O_3, and Al_2O_3 were compacted to produce environmentally beneficial composites. A pressure of 10 MPa yielded optimal mechanical properties, including hardness (80.5 Shore D) and flexural strength (35.84 MPa). Electron microscopy and thermal analysis confirmed the structural integrity and effectiveness of the filler (Manalu *et al.* 2024).

ABS-honeycomb polyester composites reinforced with sun hemp fiber and rubber seed husk cellulose exhibit exceptional flexural strength (209 MPa), tensile strength (7.7 GPa), and impact resistance (5.8 J). The enhanced matrix bonding was validated by SEM (Mahendran *et al.* 2024). The tensile, flexural, and inter-laminar shear strengths of the assessed forms were maximized in bast fiber bio-composites derived from sun hemp, measuring 71.3 MPa, 95.1 MPa, and 9 MPa, respectively (Olatunbosun *et al.* 2025). Composites including sun hemp and ABS, augmented with silane-treated rubber seed husk cellulose, exhibited outstanding performance in 3D printed structures. RSC5 demonstrated a remarkable impact energy of 13.7 J, whereas RSC4 attained tensile and flexural strengths of 142 MPa and 242 MPa, respectively. SEM confirmed the existence of filler dispersion and strong interfacial bonding (Tharanitharan *et al.* 2025). Polyester composites using sun hemp and flax fibers exhibited both hardness and dimensional stability—engineered materials exhibiting enhanced environmental durability due to reinforcing (Krishna *et al.* 2025). The tensile strength of sun hemp hessian cloth composites in high-density polyethylene (HDPE) increased by 14-42% following gamma irradiation (5 kGy), achieving 68 MPa. Both hydrophobicity and crystallinity were enhanced. SEM confirmed the strong adhesion and crosslinking between the fiber and matrix (Shohrawardy *et al.* 2024).

Although natural fiber–reinforced composites with nano-Al_2O_3 have been investigated, most prior studies concentrated on single-fiber systems or combinations with synthetic reinforcements, leaving hemp–kenaf hybrids relatively less explored. In addition, earlier works primarily emphasized tensile or flexural properties, with limited attention to interlaminar shear strength (ILSS), which is essential for understanding fiber–matrix adhesion and interlayer load transfer. The novelty of the present study lies in addressing this gap by developing hemp–kenaf–epoxy hybrid composites reinforced with nano-alumina and systematically evaluating their mechanical performance, including ILSS as a relatively novel characterization for this material system, supported by microstructural analysis to establish fiber–matrix interaction.

Table 1. Properties of the hemp, kenaf fibers, epoxy and alumina particles

S. No.	Physical Properties	Hemp Fiber	Kenaf Fiber	Epoxy Resin	Alumina
1	Density (g/ cm^3)	1.45-1.55	1.2-1.45	1.15-1.25	3.8-3.9
2	Diameter of Fiber bundle (mm)	5-20	0.05-0.12	-	-
3	Tensile Strength (MPa)	550-900	150-930	60-85	200-400
4	Youngs Modulus (GPa)	30-70	20-53	2.5-4.5	300-380
5	Elongation at break load (%)	1.6-2.2	1.5-3.3	1.5-6.0	0.01-0.02

2. MATERIALS AND METHODOLOGY

2.1 Materials

Fiber Source Enterprises of Chennai, India, supplied the hemp and kenaf fibers. From Matrix Enterprises in Nagercoil, Tamil Nadu, India, we obtained alumina nanoparticles that were 30 nm in size, 3.8 g/cm^3 in density, 9 on the hardness scale, and 300 to 380 GPa in modulus of elasticity. Adding Al_2O_3 nanofillers enhances mechanical strength but slightly reduces biodegradability. However, due to low filler content, the

composite remains largely bio-based and recyclable, offering longer service life and reduced waste for sustainable applications. Kovai Seenu Enterprises of Coimbatore, Tamil Nadu, India, provided the epoxy resin (LY556 grade) and the hardener (HY951 grade), which were combined in a proportion of 10:1. Physical characteristics of hemp fiber, kenaf fiber, epoxy, and alumina nanoparticles are listed in Table 1.

2.2 Chemical Treatment of Hemp and Kenaf Fibers

By dissolving NaOH pellets in 1 L of water, a 5 wt.% NaOH solution was made. According to Dash *et al.* (2022), the application of a 5% NaOH treatment to sun hemp fibers resulted in increased fiber roughness and reduced impurities. For an hour, the hemp and kenaf fibers were submerged in this mixture. It was necessary to rinse the fibers with a 5 wt% HCl solution (made by adding HCl to 1 liter of water) after soaking them to neutralize the NaOH. The next step was a full rinse with water, followed by an hour of drying in an oven set at 60°C to get rid of any residual moisture.

2.3 Fabrication of Hybrid Composite

At first, the law of mixtures was used to determine the correct amounts of hemp fiber, kenaf fiber, Al_2O_3, and epoxy resin. Hemp and kenaf fibers were coated with a determined quantity of epoxy resin to make pre-pregs. After that, they were semi-cured in an oven at 60°C for about an hour. Certain orientations were used to layer these semi-cured pre-pregs. Fiber orientation and stacking sequence critically affect stress distribution and failure modes. Unidirectional alignment ensures efficient load transfer, minimizes matrix cracking, and enhances tensile and flexural strength. When combined with nanofillers, unidirectional fibers achieve superior interfacial bonding and stress transfer, while random orientations increase stress concentration and early failure. To fill the spaces between the hemp and kenaf fiber mats, epoxy resin was combined with Al_2O_3 at weights of 0%, 2%, 4%, and 6%. To facilitate the development of a three-dimensional cross-linked network among the epoxy matrix and fiber reinforcements, the composite assembly was heated to 120°C and compressed to 1 MPa using a portable hot-press machine.

Five test samples were prepared for each composite composition in accordance with ASTM requirements. Table 2 provides a summary of the sample codes along with their respective compositions. In this abbreviated method, "C" stands for alumina-containing composites and the numerals 0 through 6 indicate the nano filler's weight proportion. Fig. 1 shows the various steps used to make Hemp-Kenaf-epoxy hybrid composites that have Al_2O_3 nanofillers. As shown in Table 2, the proportions of hemp and kenaf fiber remained constant while the weights of alumina and epoxy resin were varied.

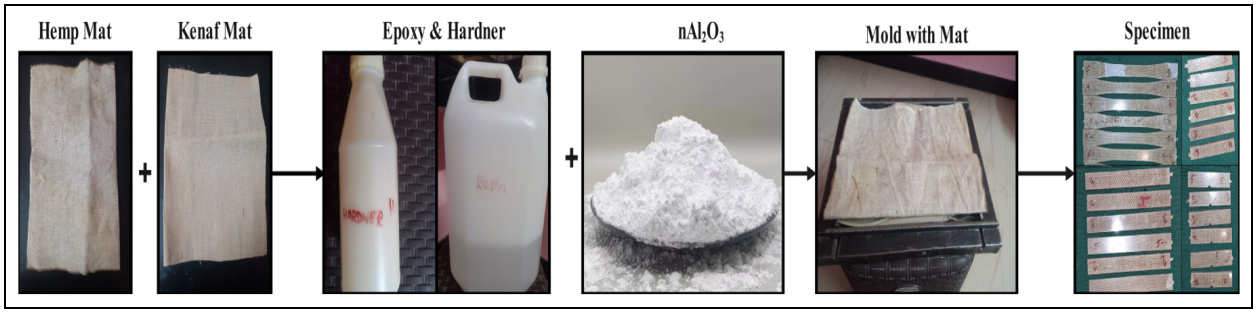


Fig. 1. Fabrication process of the composite samples

2.4 Testing of Composites

2.4.1 Tensile Test

A material's strength and deformation properties under tensile stress can be evaluated using a standardized process known as tensile testing. To accomplish consistent testing, test samples were created in accordance with the ASTM D3039 standard (ASTM D3039/D3039M-14), with dimensions of 250 mm × 25 mm x 3 mm in thickness. An Instron 1195 Universal Testing Machine, which is renowned for its precision in applying and measuring loads, was used to conduct the testing (Fig. 2). The machine has a load capacity of 5 kN. To evaluate qualities such as offset yield strength and ultimate tensile strength, the machine captures data on both the load and the elongation until the sample fails. The tensile strength of the composite sample can be determined using the following equation (1):

$$\sigma = \frac{F}{A} \quad \ldots (1),$$

where "σ" represents the tensile strength (N/mm^2), "F" is the maximum tensile load at failure (N), and "A" is the cross-sectional area of the sample (mm^2). The tensile strain was determined using equation (2).

$$E = \frac{\sigma}{\varepsilon} q \quad \text{... (2),}$$

where "E" represents the tensile strain, and "E" represents the tensile modulus (N/mm^2).

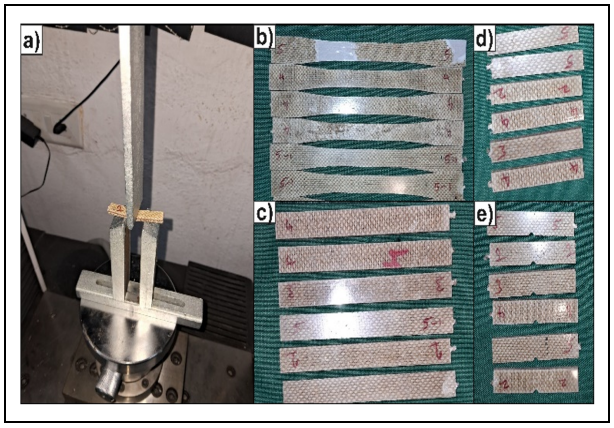


Fig. 2: (a) Universal testing machine specimen of (b) tensile test (c) flexural test (d) ILSS and (e) impact test

Table 2. Composition of the composites

Sample Code	Hemp Fiber (wt%)	Kenaf Fiber (wt%)	Alumina (wt%)	Epoxy Matrix (wt%)
C1	25	25	0	50
C2	25	25	2	48
C3	25	25	4	46
C4	25	25	6	44

2.4.2 Flexural Test

When assessing the mechanical characteristics of polymer composites subjected to bending forces, ASTM D790 (ASTM D790-03) was used for flexural testing, also known as three-point bending. The Instron 1195 Universal Testing Machine, selected for its accuracy in load application and measurement, was used to conduct the testing. It has a capacity of 5kN. The sample dimensions for the Hemp-Kenaf fiber hybrid composites were 125 mm × 3 mm × 12.7 mm, with a support span of 100 mm. Important information regarding the composite's bending ability is derived from this test, which determines its maximum stress capacity before to failure.

To determine the composite sample's flexural strength, the equation (3) was utilized:

$$p_b = \frac{3FL}{2bt^2} \quad \text{… (3),}$$

where σ_x represents the flexural strength (N/mm^2), "F" is the maximum load at failure (N), "L" is the span length of the sample (mm), and "b" and "t" are the width and thickness of the sample (mm), respectively.

The equation used to calculate the flexural modulus of the composite sample is given by equation (4).

$$E_b = \frac{mL^3}{4bt^2} \quad \text{… (4),}$$

where "E_b" represents the flexural modulus (N/mm^2), and "m" is the slope of the tangent to the initial straight-line portion of the load-deflection curve (N/mm).

2.4.3 Interlaminar Shear Strength (ILSS) Test

To determine the shear strength between composite material layers, the ILSS test was conducted in accordance with ASTM D2344 standard. Samples that are cut to 64 mm × 10 mm × 3 mm are subjected to a conditioning process at 23℃ and 50% relative humidity. Because of its reliability in load application and measurement, the Instron 1195 Universal Testing Machine was selected to carry out the tests. The machine has a capacity of 5 kN. A three-point bending fixture was used with a support span of 12 mm, which is four times the sample thickness. The loading nose and supports both had radii of 5 mm. The failure occurred within 1 to 2 minutes due to the load being applied at a rate of 2 mm/min.

To determine the interlaminar shear strength (ILSS) of composite sample's, the following formula equation (5) was used.

$$ILSS = \frac{3F}{4bt} q \quad \text{… (5),}$$

where "F" represents the maximum load at failure (N), and "b" and "t" are the width and thickness of the sample (mm), respectively.

2.4.4 Impact Test

The impact properties of the composite were assessed using the Zwick-Rowell Izod testing apparatus. The Izod impact test method is described in ASTM D256, which is used to evaluate the impact resistance of composites made of a polymer matrix. The test samples of the hybrid composite made of hemp and kenaf fibers were 12 mm × 3 mm × 64 mm. The samples were placed on a vertical mount and subjected to impact testing at one end. The following formula was used to determine the impact strength based on the energy absorbed during the impact:

$$\text{Impact Strength} = \frac{\vec{E}_i}{t} \quad \text{… (6)}$$

where E_i represents the impact energy (J), and t is the thickness of the sample (mm). This test evaluates the material's toughness and resistance to fracture under sudden forces.

2.4.5 Hardness Test

Digital Rockwell hardness testers were used to determine the hardness of electrical insulating materials and polymers in accordance with ASTM D785 (ASTM D785-98). The hybrid composite of Hemp and Kenaf fibers was tested using 3 mm thick samples. A ball indenter with a diameter of 1/4 inch and a force of 60 kg was utilized.

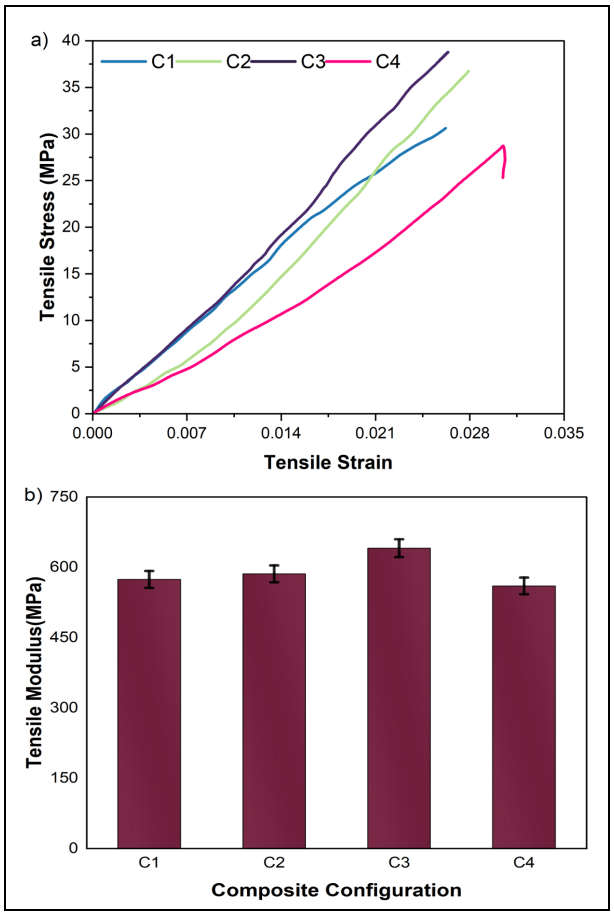


Fig. 3: (a) Tensile stress versus strain curves of various hemp-kenaf-epoxy hybrid composites and (b) tensile modulus versus composite configuration

3. RESULTS AND DISCUSSION

3.1 Tensile Test

The resulting composite was fragile and prone to catastrophic failure, as shown in Fig. 3(a) of the stress-strain curve for different Hemp-Kenaf-epoxy hybrid composites. The fact that there are no yield points before fracture proves this. The tensile stress of the C3 samples is 31% higher than that of the C2 samples, 36% higher than the C4 samples, and 28% higher than the C3 composites. The tensile modulus vs composite configuration is shown in Figure 4(b). The C3 composite outperforms the C1, C2, and C4 composites by a substantial margin, with increases of about 10%, 8%, and 12%, respectively. This indicates that the composite's tensile properties are enhanced with the addition of up to 6 wt% Al_2O_3. The addition of Al_2O_3 to the polymer matrix can alter its crystallinity, probably because the wood particles act as nucleating agents. Consequently, a more noticeable impact on tensile characteristics may be observed with higher increases in Al_2O_3 concentration. The interaction between the fibers and the matrix is impacted by this shift in crystallinity, which may reduce the interfacial adhesion of the Al_2O_3 nano filler to the matrix. Consequently, the composite's strength can drop since it cannot transfer tensile stress as well.

High tensile strength (29.94 MPa) were recorded in sisal/flax-reinforced nanocomposites treated with 5% NaOH and using green-synthesized Al_2O_3. The filler content was 4 wt% as observed by (Lakshmaiya *et al.* 2022). This dispersion is further limited by the strong hydrogen bonding between the fibers, which worsens the already reduced tensile characteristics. Hydroxyl groups in the fiber structure encourage water molecules to establish hydrogen bonds, which lowers the mechanical characteristics of the composite material as it absorbs moisture. The average and standard deviation of tensile strength and modulus for several composite configurations with varying percentages of Al_2O_3 nano filler are shown in Table 3.

Table 3. Tensile strength and modulus of various composite

S. No.	Composite Configuration	Tensile Strength (MPa) Means ± SE	Tensile Modulus (MPa) Means ± SE
1	C1	31.21 ± 32.89	574.16 ± 5.18
2	C2	36.71 ± 11.6	585.98 ± 7.17
3	C3	38.42 ± 12.29	640.94 ± 8.14
4	C4	28.32 ± 49.48	560.37 ± 3.19

3.2 Flexural Test

Fig. 4(a) displays the flexural stress and strain curves for various composite configurations, showing that the flexural strength of the C3 composite is approximately 19%, 3%, and 10% greater than that of the C1, C2, and C4 composites, respectively. Fig. 4(b) illustrates the flexural modulus for each composite configuration, indicating that C3 exhibits a higher flexural modulus with values approximately 20%, 1%, and 17% greater than those of the C1, C2, and C4 composites respectively. Fig. 4 (a) clearly shows that incorporating 4 wt% Al_2O_3 enhances the composite's flexural strength. This improvement is attributed to efficient load transfer between the matrix and reinforcement facilitated by the well-distributed clusters at the 4 wt% concentration. These clusters optimize stress distribution in the C3 sample, leading to increased flexural strength. The flexural modulus measures the

material rigidity and also improved significantly at 4 wt% (C3) concentration. The addition of rigid fibers to the softer matrix reduced matrix mobility, thereby increasing the composite's stiffness. This suggests that Al_2O_3 at this concentration strengthens the matrix, enhancing the C3 sample's ability to resist deformation under stress.

Composites composed of Ramie fibers and incorporated with varying quantities of Al_2O_3 had the maximum flexural (39.25 MPa) in the A sample. Al_2O_3 was determined to enhance mechanical properties as indicated by the investigation.(Raja *et al.* 2024). As the Al_2O_3 concentration increased, the composites showed a gradual improvement in flexural strength, likely due to increased resistance to shearing within the composite structure, attributed to the presence of fibers.

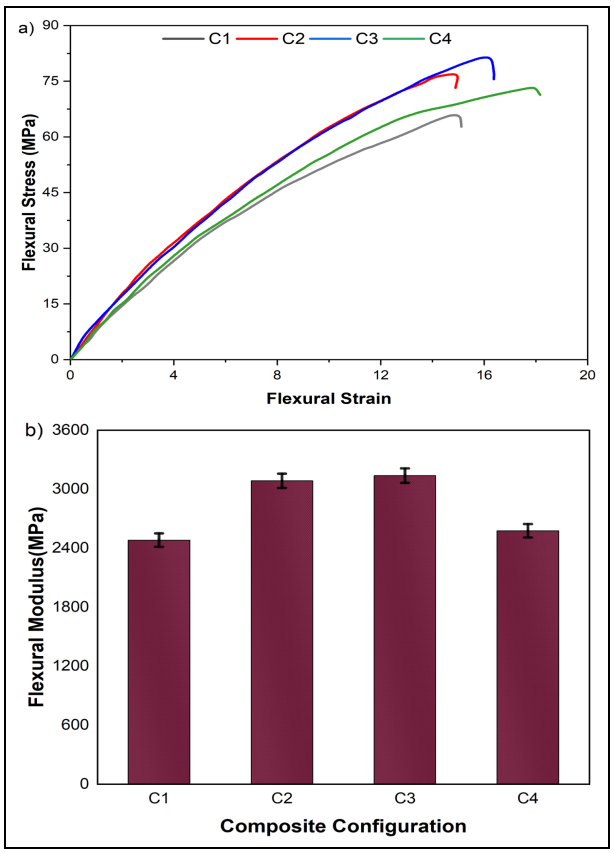


Fig. 4: (a) Flexural stress versus strain curves of various Hemp-Kenaf-epoxy hybrid composites and (b) flexural modulus versus composite configuration

Further improvements in flexural properties could be achieved by chemically treating the banana fibers and Al_2O_3. Kassa *et al.* (2025) demonstrated that chemically treated composites exhibit better resistance to bending and energy absorption. This improvement is likely due to the nature of filler, which contributes to superior mechanical properties compared to other fillers. However, further increasing the Al_2O_3 content in the composite may reduce the flexural properties.

Flexural strength and modulus, along with their respective standard errors, are displayed in Table 4 for a range of composite topologies including varying amounts of Al_2O_3 nano filler.

Table 4. Flexural strength and modulus of various composite

S. No.	Composite Configuration	Flexural Strength (MPa) Means ± SE	Flexural Modulus (MPa) Means ± SE
1	C1	62.85 ± 9.31	2482.59 ± 59.18
2	C2	74.98 ± 8.26	3086.06 ± 16.43
3	C3	57759 ± 6.63	3138.54 ± 25.27
4	C4	67.21 ± 2.06	2578.07 ± 48.06

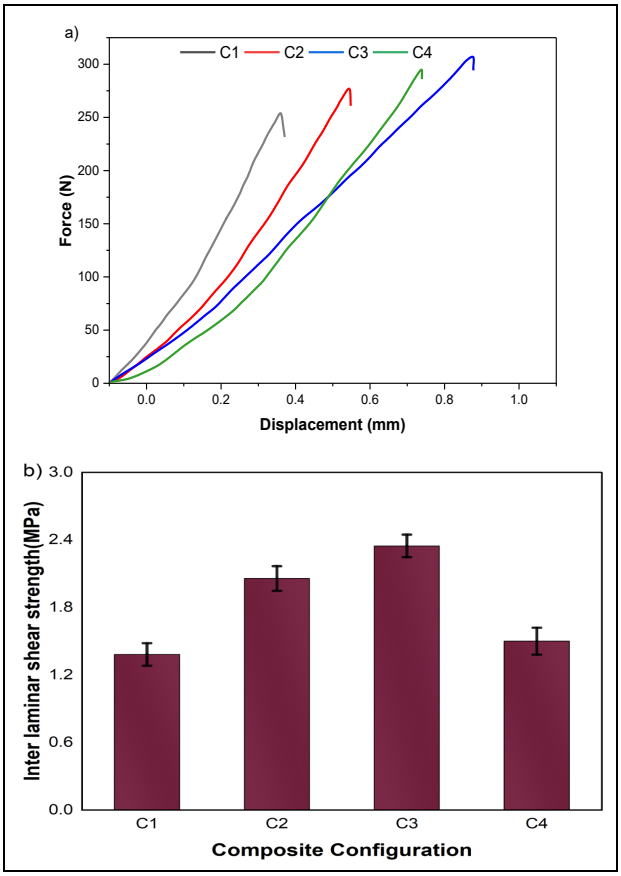


Fig. 5: (a) Force versus displacement curves and (b) ILSS of various hemp-kenaf-epoxy hybrid composites subjected to ILSS test

3.3 Interlaminar Shear Strength Test

Fig. 5(a) displays the force versus displacement curves for various composite configurations, showing that the C3 composite has a higher load-carrying capacity, approximately 16%, 10%, and 7% greater than the C1, C2, and C4 composites, respectively. Fig. 5(b) presents the ILSS of the various composite, indicating that the C3 composite exhibits a significantly higher

ILSS with values about 41%, 12%, and 26% greater than the C1, C2, and C4 composites, respectively.

The enhancement is ascribed to the 4 wt% Al_2O_3 content in the Hemp-Kenaf composite, which fills micro-voids and diminishes stress concentrations inside the material (Table 5). The ILSS strength of the C3 composite is augmented due to enhanced load transfer efficiency between the fibers and the matrix, achieved at a concentration of 4 wt%. The C1 sample utilizes epoxy resin and the characteristics of hemp and kenaf fibers in place of Al_2O_3 as a filler.

Epoxy composites with 127% grafted sun hemp fiber exhibited maximum interlaminar shear strength (68.9 MPa) as reported by Jadhav and Jadhav (2022), indicating a significant enhancement in fiber-matrix adhesion and overall load transfer efficiency within the composite structure.

Table 5. Maximum applied load and interlaminar shear strength of various composite

S. No.	Composite Configuration	Maximum Load (N) Means ± SE	ILSS (MPa) Means ± SE
1	C1	252 ± 12.63	1.38 ± 7.72
2	C2	270 ± 13.28	2.05 ± 5.129
3	C3	302 ± 18.64	2.34 ± 4.816
4	C4	280 ± 17.54	1.50 ± 2.41

3.4 Impact Test

Figure 6(a) depicts the correlation between absorbed energy and composite configuration. The C3 composite absorbs more energy upon impact than the C2 and C4 composites, with increases of around 24%, 22%, and 6%, respectively. C3 has enhanced impact strength relative to C1, C2, and C4 composites, with increases of approximately 12%, 9%, and 18%, respectively, as depicted in Figure 6(b), which illustrates the correlation between impact strength and composite configuration.

Table 6 shows the absorbed energy and impact strength of various composite. At 4 wt% Al_2O_3, the material functions as a nano filler, absorbing impact energy and enhancing load transfer efficiency between the matrix and fibers. The reduced impact strength is attributable to an increase in micro-cracks or voids and insufficient load transfer between the matrix and fibers in C1 samples without Al_2O_3 nano filler. The incorporation of 2 wt% Al_2O_3 into the mixture improved impact strength by strengthening the composite, reducing fracture propagation sites, and increasing energy dissipation. At 6 wt% Al_2O_3 (C4), the impact strength diminishes considerably. Multiple factors affect the impact strength. This includes the longevity of the reinforcement, surface roughness, contact dynamics, and the effort needed to remove nano filler particles from the matrix owing to friction. As demonstrated by Herlina *et al.* (2024) hybrid composites comprising 30% *Paederia foetida* fiber and 10% Al_2O_3 exhibited an impact strength of 24 kJ/m^2, outperforming other formulations in terms of toughness and resistance to crack propagation.

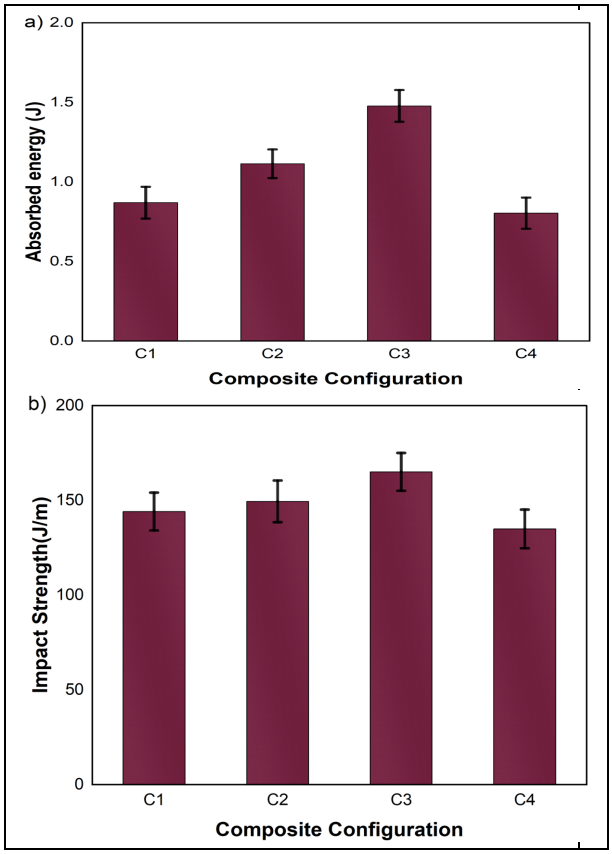


Fig. 6: (a) absorbed energy of different composite and (b) impact strength of various composite

Table 6. Absorbed energy and impact strength of various composite

S. No.	Composite Configuration	Absorbed Energy (J) Means ± SE	Impact Strength (MPa) Means ± SE
1	C1	0.86 ± 0.0372	144 ± 6.81
2	C2	1.11 ± 0.0253	149.46 ± 12.37
3	C3	1.47 ± 0.423	134.91±17.83
4	C4	0.80 ± 0.0379	134.91 ± 9.65

3.5 Hardness Test

Fig. 7 displays the hardness values for several composite combinations. The C3 composite exhibits a hardness that is approximately 20% greater than C1, 7% greater than C2, and 5% greater than C4. All hardness values are presented in Table 7. The interplay between Hemp-Kenaf fibers and the epoxy matrix affects the composite's hardness. The C1 sample devoid of Al_2O_3

filler is completely inflexible. An increased Rockwell Hardness number arises from enhanced load transfer efficiency, which is somewhat augmented by the addition of 2 wt% Al_2O_3 nano filler (C2). Elevating the alumina concentration to 4 wt% (C3) improves the density and reinforcing properties of the composite, hence increasing its hardness. If the interaction between the nanofiller and matrix reaches an ideal condition, further development may become impractical.

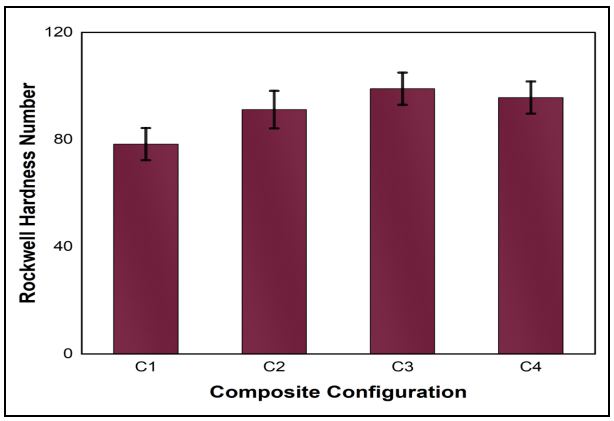


Fig. 7: Rockwell hardness number of composite samples

The reduced hardness at 6% Al_2O_3 (C4) is attributable to agglomeration and inadequate dispersion, which may lead to micro-cracks and regions of stress concentration. With an increase in fiber loading, the composites demonstrate enhanced hardness. The decline in hardness and impact strength at higher Al_2O_3 loadings is mainly due to nanoparticle agglomeration, which creates microvoids and localized stress concentrations. These weak zones hinder effective stress transfer, initiate microcracks, and reduce the composite's ability to resist indentation and absorb impact energy. The decrease in voids, enhanced interfacial adhesion between the fibers and the matrix, and more consistent distribution of the nano filler inside the matrix all facilitate this enhancement. Fig. 7 depicts the average values and standard errors of the Rockwell hardness number for several composite with varying weight percentage of Al_2O_3 nano filler. The improved hardness properties arise from the composites' reduced flexibility and improved rigidity. According to the author (Taj *et al.* 2023), Kenaf/epoxy composites reinforced with 0.6% nano-Al_2O_3 and 0.3% nanographene demonstrated enhanced mechanical properties, with the optimal formulation of 6% Al_2O_3 and 3% graphene attaining a peak hardness of 27 HV, underscoring the synergistic effect of dual nanofiller integration on improving the composite's structural integrity.

3.6 SEM Analysis

Fig. 8 depicts the fracture surface morphology of fiber-reinforced composites with differing Al_2O_3 nanofiller content, emphasizing its effect on fiber-matrix adhesion and mechanical properties. Fig. 8(a) illustrates considerable fiber pull-out, signifying inadequate interfacial bonding in the C1 sample, where the lack of appropriate nanofillers leads to debonding under tensile stress. Fig. 8(b) similarly exhibits negligible fiber interaction (C2 sample) and a smooth matrix surface, indicating that a modest concentration of nanofiller is insufficient to improve adhesion. The integration of *Pisum sativum* nanocellulose and silane-modified sun hemp fiber into polyester composites, due to improved matrix-filler interaction and dispersion, as verified by SEM analysis (Alshahrani and Prakash, 2025). Conversely, Fig. 8(c), depicting the C3 sample with 4 wt% Al_2O_3, nano filler exhibits minimal fibrillation and micro-cracking, indicating enhanced fiber-matrix adhesion attributed to the uniform distribution of nanofillers, hence augmenting mechanical strength. Fig. 8(d) (C4 sample with 6 wt% nanofiller) illustrates a porous structure resulting from the agglomeration of surplus nanofillers, which leads to inadequate adhesion and diminished mechanical characteristics. These data affirm that an optimal nanofiller concentration (about 4 wt%) is essential for improving composite performance, whereas insufficient or excessive amounts result in interfacial failure and structural deterioration.

Table 7. Rockwell hardness number of various composite

S. No.	Composite Configuration	Means ± SE
1	C1	78.33 ± 5.18
2	C2	91.21 ± 8.60
3	C3	98.98 ± 6.93
4	C4	95.69 ± 5.79

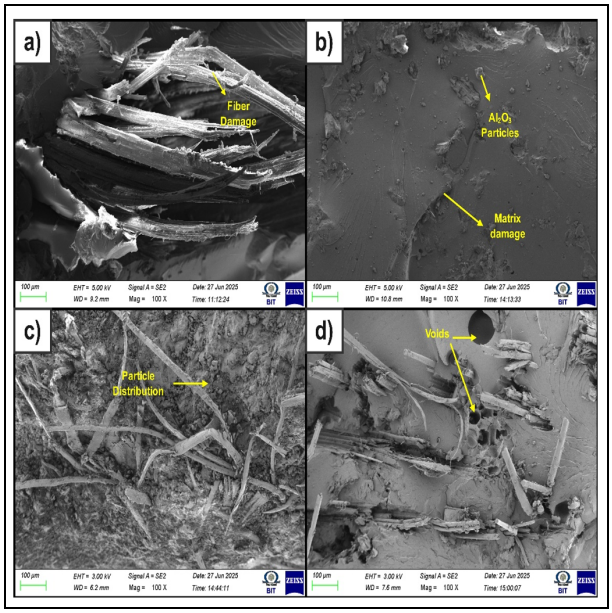


Fig. 8: Microstructural analysis of the fractured surfaces of samples subjected to loading, corresponding to (a) C1, (b) C2, (c) C3 and (d) C4

4. CONCLUSION

The hemp–kenaf–epoxy hybrid composite reinforced with Al_2O_3 nanofiller exhibited significant improvements in mechanical performance, with the 4 wt% Al_2O_3 (C3) composition achieving the best balance of properties. Compared with the unfilled and low-filler composites, C3 showed notable gains in tensile and flexural properties, interlaminar shear strength, impact resistance, hardness, and energy absorption due to improved nanoparticle dispersion, stress distribution, and load transfer. Filler contents above 6 wt% led to agglomeration, inducing microcracks and stress concentrations that degraded performance. The composite outperformed automotive-grade plastics and offers a sustainable alternative for applications demanding high mechanical strength, including impact-critical uses. The hemp-to-kenaf ratio was kept constant to isolate nanofiller effects. Future work should optimize fiber ratios and evaluate long-term durability through environmental conditioning and thermal cycling.

FUNDING

This research received no specific grant from any funding agency in the public, commercial, or not-for-profit sectors.

CONFLICTS OF INTEREST

The authors declare that there is no conflict of interest.

COPYRIGHT

This article is an open-access article distributed under the terms and conditions of the Creative Commons Attribution (CC BY) license (http://creativecommons.org/licenses/by/4.0/)

REFERENCES

Alshahrani, H. and Prakash, V. R. A., Characterisation of microcrystalline cellulose from waste green pea pod sheath and its sun hemp fibre-polyester composite: A step towards greener manufacturing, *Physiol. Plant.,* 176(1), e14166(2024). https://doi.org/10.1111/ppl.14166

Alshahrani, H. and Prakash, V. R. A., Characterisation of Nanocellulose from Waste Pisum Sativum Sheath and its Sun Hemp Fibre-Polyester Composite: A Step Towards Valorisation of Biomass, *Waste Biomass Valorization*., 16(4), 1999–2010(2025). https://doi.org/10.1007/s12649-024-02794-9

Amjad, A., Abidin, M. S. Z., Alshahrani, H. and Rahman, A. A. A., Effect of fibre surface treatment and nanofiller addition on the mechanical properties of flax/pla fibre reinforced epoxy hybrid nanocomposite, *Polym*., 13(21), 3842(2021). https://doi.org/10.3390/polym13213842

Amjad, A., Rahman, A. A. A. and Abidin, M. S. Z., Effect of Nanofillers on Mechanical and Water Absorption Properties of Alkaline Treated Jute Fiber Reinforced Epoxy Bio Nanocomposites, *J. Nat. Fibers*., 19(16), 14592–14608(2022). https://doi.org/10.1080/15440478.2022.2068171

Arunachalam, S. J., Saravanan, R., Othman, N. A., Thanikodi, S., Giri, J., Azizi, M. and Saidani, T., Artificial Intelligence-Driven Prediction and Optimization of Tensile and Impact Strength in Natural Fiber/Aluminum Oxide Polymer Nanocomposites, *Eng. Rep.,* 7(4), (2025). https://doi.org/10.1002/eng2.70093

Bharathi, M., Kumaran, S. S. and Samson, P. E., Effect of silica nanoparticles on mechanical and thermal properties of intra-inter ply hybrid laminated composites, *Mater. Res. Express.,* 8(4), 045306(2021). https://doi.org/10.1088/2053-1591/abf530

Dash, C., Das, A. and Bisoyi, D. K., High-Intensity Ultrasonication (HIU) Effect on Sun Hemp Fiber-Reinforced Epoxy Composite: A Physicochemical Treatment Toward Fiber, 1st Ed., Natural Polymers, *Apple Academic Press,* 193–224(2022). https://doi.org/10.1201/9781003130765-8

Edlabadkar, A. P., Madhu, M. C., Arunbharathi, R., Sharma, D., Singh, N., Revathi, R. and Mayakannan, S., Optimization of Mechanical Properties of Cordia dichotoma/Alumina Nanoparticle Reinforced Epoxy Nanocomposites Under Alkali Treatment Using ANN Techniques*, J. Environ. Nanotechnol.,* 14(2), 525–540(2025). https://doi.org/10.13074/jent.2025.06.2521549

Haile, D., Mengesha, G. A., Sinha, D. K., Kebere Aschenaki, H. and Beshahwured, S. L., Effect of bamboo powder on mechanical property of aluminum matrix composite reinforced with aluminum oxide, boron carbide and molybdenum disulfide, *Adv. Mech. Eng*., 16(1), 16878132231221646(2024). https://doi.org/10.1177/16878132231221646

Harak, S. S., Krishnaveni, K., Karthick, K., Chinnarasu, K., Prasad, P. V. H., Tonk, A. and Mayakannan, S., Experimental Study on the Mechanical Properties of Hybrid Areca and Abaca Fiber Reinforced Polymer Composites, *J. Environ. Nanotechnol.,* 13(4), 92–101(2024). https://doi.org/10.13074/jent.2024.12.244977

Herlina, S. N., Suteja, S., Pruncu, C. I., Setyawan, I., Ilyas, R. A. and Lamberti, L., Physicomechanical, water absorption and thermal properties and morphology of Paederia foetida fiber–Al2O3 powder hybrid-reinforced epoxy composites, *Polym. Int*., 73(7), 573–585(2024). https://doi.org/10.1002/pi.6632

Jadhav, A. C. and Jadhav, N. C., Waste sun hemp fibres/epoxy composites: mechanical and thermal properties, *Iran. Polym. J.,* 31(7), 821–833(2022). https://doi.org/10.1007/s13726-022-01034-y

Jayabalakrishnan, D., Kumar, S. S., Madhu, S. and Bhaskar, K., Flame retardant, load bearing and thermal studies on satin weaved sun hemp fibre and cashew nut shell de-oiled cake biosilica epoxy composites, *Biomass Convers. Biorefin.,* 14(17), 21085–21093(2024). https://doi.org/10.1007/s13399-023-04055-6

John, P. K. A., Ravikumar Solomon, G., Sivakumar, S., Sathish, S. and Viswanathan, K., Effect of rosin and flax fibers on the improvement in mechanical properties of hybrid polymeric composites. International Journal of Mechanical and Production *Eng. Res. Develop*., 10(2), 867–878(2020).

Krishna, V. N., Elango, M., Krishnan, T. and Jayabal, S., Tensile, Flexural and Impact Properties of Hybrid Sunhemp-Flax Fiber Based Thermosetting Composites, *J. Nat. Fibers.,* 19(15), 10737–10745(2022). https://doi.org/10.1080/15440478.2021.2002765

Krishna, V. N., Sivasankaran, R., Prasad, S. D. and Govardhanan, M. S., Hybrid Polyester Composites Reinforced with Sun Hemp and Flax Fibres: Shore D Hardness and Dimensional Stability Analysis, *Trans. Famena.,* 49(1), 15–24(2025). https://doi.org/10.21278/TOF.491055423

Lakshmaiya, N., Ganesan, V., Paramasivam, P. and Dhanasekaran, S., Influence of Biosynthesized Nanoparticles Addition and Fibre Content on the Mechanical and Moisture Absorption Behaviour of Natural Fibre Composite, *Appl. Sci.,* 12(24), 13030(2022). https://doi.org/10.3390/app122413030

Mahendran, G., Mageswari, M., Kakaravada, I. and Rao, P. K. V., Characterization of polyester composite developed using silane-treated rubber seed cellulose toughened acrylonitrile butadiene styrene honey comb core and sun hemp fiber, *Polym. Bull*., 81(17), 15955–15973(2024). https://doi.org/10.1007/s00289-024-05427-2

Manalu, J., Numberi, J. J., Safanpo, A., Fitriyana, D. F., Wijaya, T. L., Siregar, J. P., Cionita, T. and Jaafar, J., Characterization of eco-friendly composites for automotive applications prepared by the compression molding method, *Polym. Compos*., 45(9), 8104–8118 (2024). https://doi.org/10.1002/pc.28327

Mayakannan, S., Raj, J. B., Raja, V. L. and Nagaraj, M., Effectiveness of silicon nanoparticles on the mechanical, wear, and physical characteristics of PALF/sisal fiber–based polymer hybrid nanocomposites, *Biomass Convers. Biorefin.*, 13(14), 13291–13305(2023). https://doi.org/10.1007/s13399-023-04654-3

Olatunbosun, B., Manalo, A., Aravinthan, T., Chen, G. and Kiriella, S., Modelling of manufacturing parameters and characterisation on the mechanical properties of sun hemp (*Crotalaria juncea L.*) bio-composites with different fibre forms,s *Constr. Build. Mater.,* 489, 142349(2025). https://doi.org/10.1016/j.conbuildmat.2025.142349

Raj, H., Choudhury, A. M., Tripathi, S., Bauri, S., Mandal, S. S., Prakash, R., Tiwari, S., Layek, R. K. and Maiti, P., Sun hemp reinforced poly (lactic acid) green composites: Controlled biodegradation and improved fracture toughness through interlocking mechanism, *Ind. Crops Prod*., 223, 120245(2025). https://doi.org/10.1016/j.indcrop.2024.120245

Raja, T., Vinayagam, M., Venkataramanan, A. R., Mohankumar, A., Chinnathambi, A., Alharbi, S. A. and Kalam, M. A., Effect of nano alumina particles on Boehmeria nivea fiber-reinforced polyester green composite: biological, elemental and mechanical analysis, *Opt. Quantum Electron*., 56(4), 538(2024). https://doi.org/10.1007/s11082-023-06188-4

Rakeshkumar, C., Surenderpaul, A., Naveen, R. and Kumar, A. S., Effect of chemical treatment on mechanical properties of prosopis juliflora fibre and glass fiber with nano fillers, *Mater. Today Proc*., , S221478532301(2023). https://doi.org/10.1016/j.matpr.2023.03.398

Kumar, M. S., Sivakumar, M., Senthil, S. M. and Rajeshkumar, L., Effect of alumina fillers on physical and mechanical properties of luffa/groundnut shell natural fiber reinforced polymer composites, *Polym. Compos*., 45(11), 10457–10469(2024). https://doi.org/10.1002/pc.28487

Shohrawardy, M. H. S., Mina, M. F., Alam, A. K. M. M., Khan, R. A. and Hossain, M. M., Effects of chemical treatment and gamma-ray irradiation on the structure-properties of sun hemp and okra hessian cloth reinforced high-density polyethylene composites: A comparative study, *J. Thermoplast. Compos. Mate*r., 37(12), 3735–3764(2024). https://doi.org/10.1177/08927057241239941

Subbiah, A., Chockalingam, P., Munimathan, A. and Mayakannan, K., Effect of fiber orientation on interlaminar shear stresses and thermproperty of sisal fiber reinforced epoxy composites, *Rev. Mater.,* 29(4), e20240491(2024). https://doi.org/10.1590/1517-7076-rmat-2024-0491

Taj, A., Swamy, R. P., Naik, K. and Bharath, K. N., An evaluation on mechanical properties of vaccum bagging processed kenaf epoxy nano aluminium oxide and nanographene composites, *Eng. Res. Exp*., 5(2), 025007(2023). https://doi.org/10.1088/2631-8695/acc996

Tavadi, A., Basheer, D., Melese, K. G., Kumaresan, K., Mohan, N., Kerur, M. R. H. and Shashidhara, L. C., Experimental analysis of mechanical properties and FTIR analysis of areca fiber-reinforced epoxy composites incorporating Al2O3, *J. Ind. Text.,* 55, 15280837241313217(2025). https://doi.org/10.1177/15280837241313217

Tharanitharan, G., Saravanan, C., Raja, P. and Ajaykarthik, R. T., Investigation of temperature and water aging effects on epoxy composites reinforced with natural fibers and surface-modified cellulose filler, *Polym. Bull.,* 82(10), 4621–4647(2025). https://doi.org/10.1007/s00289-025-05682-x